Surface-induced orientational order in the isotropic phase of a liquid-crystal material

G. P. Crawford, R. Stannarius,* and J. W. Doane
Liquid Crystal Institute and Department of Physics, Kent State University, Kent, Ohio 44242-0001
(Received 26 February 1991)

Orientational order in the isotropic phase of liquid crystals confined to 0.2-μm-diam cylindrical channels of Anopore membranes is measured by deuterium nuclear magnetic resonance. At temperatures deep in the isotropic phase, the measurements reveal the order of the first molecular layer at the cavity wall, while at temperatures near the isotropic-nematic transition the measurements are primarily sensitive to order penetrating into the cavity in a manner described by the Landau–de Gennes theory. The degree of order S_0 at the cavity wall is measured and the surface coupling constant determined for various treatments of the cavity wall. Wide variations of S_0 are found for different surface treatments. Treatments that yield both perpendicular and parallel molecular anchoring are explored. The angular dependence of the surface-induced nematic order is investigated following the $P_2(\cos\theta)$ expression independent of molecular anchoring at the surface.

I. INTRODUCTION

The orienting mechanisms that govern the interaction between a liquid-crystal molecule and a solid substrate are an important topic in the physics of interfacial phenomena. These mechanisms can be classified into two categories: short-range substrate-fluid anisotropic interactions generally chemical in nature, and long-range fluid-fluid anisotropic interactions resulting from liquid-crystalline properties. Several theories based on Landau–de Gennes formalism [1–5], Maier-Saupe [6], and molecular approaches [7] have been developed to describe orientational ordering near a solid surface. The value of the orientational order parameter at the surface is a direct measure of the anisotropic substrate-fluid potential. For a certain strength of surface interactions, an orientated interfacial boundary layer (prewetting transition) is predicted to occur [1,2,6].

Several experimental studies have been performed to measure the orientational order parameter at the surface. Miyano [8] first pioneered a method to investigate the aligning forces at a liquid-crystal–solid interface by observing wall-induced pretransitional birefringence above the nematic-isotropic transition (*N-I*). Using the Landau–de Gennes theory, several surfaces order parameters were reported for 5CB and MBBA [N-(*p*-methoxybenzylidene)-*p'*-butlylaniline] for various surface treatments. Shen *et al.* [9] have employed evanescent-wave-ellipsometry techniques on homeotropically aligned planar samples for the homologous series of alkyl cyanobiphenyls (*n*CB). The substrate was kept unchanged and the hydrocarbon chain length was varied to effectively alter the liquid-crystal–solid-substrate interaction in a systematic way. It was also shown by Shen [10] that surface second-harmonic generation (SHG) can be used to probe the orientational anisotropy of liquid-crystal monolayers. Other studies of liquid-crystal–substrate interactions include field-induced twist [11], combined optical and capacitance measurements [12], and small-angle x-ray scattering [13]. Recently we discovered that deuterium nuclear magnetic resonance (^{2}H-NMR) of liquid crystals confined to the cylindrical cavities of Nuclepore filters is quite sensitive to orientational order imposed by the cavity walls [14]. This order could be observed at temperatures deep into the isotropic phase, some $\sim 20\,^{\circ}$C above the nematic-isotropic transition temperature $T_{N\text{-}I}$. It was found that the traditional theoretical approaches described above could not explain this behavior over the broad range of temperatures. We found, however, that the data could be explained if the orientational order of the first molecular layer at the cavity wall was governed by weakly temperature-independent local molecular interactions with the remaining order which penetrates into the cavity following the Sheng theory. From NMR measurements, it was further discovered that the molecular exchange rate between the surface layer and the bulk was $\sim 10^3\ s^{-1}$, substantially slower than the rate of molecular exchange in the bulk. This further indicated that the interaction between the surface layer and the wall was local in nature.

In this contribution we expand upon these ^{2}H-NMR studies to explore the effect that different surface treatments have upon surface-induced order. Our experimental studies are carried out in the 0.2-μm-diameter channels of Anopore membranes that were filled with the liquid-crystal material 4′-*n*-pentyl-4-cyanobiphenyl deuterium labeled on the second position of the hydrocarbon chain (5CB-βd_2). The high surface-to-volume ratio exhibited by these membranes make it possible for ^{2}H-NMR to directly observe surface-induced order. A scanning-electron-microscopic photograph of the Anopore membrane is presented in Fig. 1. The rigid structure and chemical compatibility of the membrane allow the cavity walls to be treated with surfactants and polymers in a systematic way to investigate the effect on the interfacial parameters. The small size of the cavities in these filters further allows us to simplify the analysis of

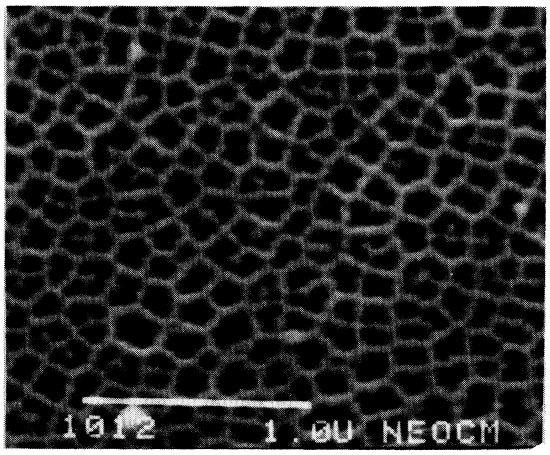

FIG. 1. Scanning-electron-microscope photograph of an Anopore inorganic membrane with pores of diameter 0.2 μm. The scale shown in the photograph represents 1 μm.

the ^{2}H-NMR data in that during the long time scale of the NMR measurement (milliseconds) a diffusing molecule samples the order throughout the cross section of the cavity (fast motional averaging regime). The quadrupolar NMR splitting from a deuterated segment of the molecule can be expressed in closed form as the sum of two terms that describe the local order at the surface governed by substrate-fluid interactions and the decay of order away from the surface resulting from fluid-fluid anisotropic interactions. From this analysis we obtain as fitting parameters the order S_0 of the first molecular layer and a parameter l_0, which is representative of the interfacial layer thickness [14]. From the values of S_0, values of the substrate-fluid interaction, often referred to as the surface coupling constant, can be calculated. The data from different surface treatments show that wide variations in S_0 and the surface coupling constant are possible.

We present a novel approach to the determination of the molecular orientational order parameter at the surface of a solid substrate. By performing temperature-dependence experiments in the isotropic phase, two surface parameters S_0 and l_0 are directly obtained from the experimental data. Applying various surface treatments to the cavity walls, the anchoring conditions at the surface and the value of the anisotropic substrate-fluid potential are altered. We have determined that the surface order parameter can be temperature dependent or temperature independent, depending on the nature of surface interactions controlled by the preparation of the cavity wall. These studies were motivated by their relevance to basic physics [1–14] and to further the understanding of finite-size effects that are utilized in many liquid-crystal devices [15].

II. THEORY

We employ the Landau–de Gennes formalism for the N-I transition that is used to give a phenomenological expression for the free-energy density [16,17]. The liquid-crystal material is assumed to be confined to a cylindrical cavity of radius R. We have considered the profile of nematic order away from the cavity wall with a rotational symmetry and translational symmetry along the cylinder axis. For systems with a uniform director orientation, the free-energy density can be expanded in terms of a single order parameter expressed as

$$f = f_0 + f_1[S(r)] + \frac{L}{2}[\nabla S(r)]^2 - GS(r)\delta(r) , \tag{1}$$

$$f_1[S(r)] = \frac{a}{2}(T - T^*)S^2(r) - \frac{B}{3}S^3(r) + \frac{C}{4}S^4(r) , \tag{2}$$

where f_0 is the order-parameter-independent part of the free-energy density, r is the distance from the cylindrical axis, and a, B, C, L, and T^* are material parameters. The final term in Eq. (1) is the surface free-energy density first introduced by Sheng [2]. This term incorporates an uniaxial aligning potential in the vicinity of the surface experienced by the liquid-crystal molecule where G reflects the strength of the interaction. The interaction between the molecules and the surface is short range as evident of the δ function. The total free energy is obtained by integrating Eq. (1) over the volume of the sample and is given by

$$F = \int_{\text{vol}} \left[f_0 + f_1[S(r)] + \frac{L}{2}[\nabla S(r)]^2 \right] dV - \tfrac{1}{2} G A S_0 , \tag{3}$$

where S_0 is the order parameter at the surface and A is the surface area.

The equilibrium form of $S(r)$ can be obtained by the minimization of F given in Eq. (3). The minimization procedure is a two-step process. First, we calculate the function $S(r)$ for a given boundary value S_0, then Eq. (1) is minimized according to the variational principle with respect to $S(r)$. If we neglect $S^3(r)$ and $S^4(r)$ terms, which is justified in the isotropic phase and an approximation for surface-induced order, the solution for the orientational order parameter in the bulk as a function of distance away form the cavity wall is expressed as

$$S(r) = S_0 \frac{\cosh(r/\xi)}{\cosh(R/\xi)} , \tag{4}$$

where R is the radius of the cavity and ξ is the correlation length given by

$$\xi = \left[\frac{L}{a(T - T^*)} \right]^{1/2} = \xi_0 \left[\frac{T^*}{T - T^*} \right]^{1/2} , \tag{5}$$

where ξ_0 is the standard temperature coherence length defined by $\xi^2 = L/(aT^*)$. The order parameter at the cylinder axis, $S(r=0) = S_m$, is given by

$$S_m = \frac{S_0}{\cosh(R/\xi)} . \tag{6}$$

If the size of the cavity is much larger than the correla-

tion length ($\xi \ll R$), Eq. (4) can be reduced to the simple exponential form given by

$$S(r)=S_0 e^{-(R-r)/\xi} , \tag{7}$$

with $S_m \sim 0$. The second minimization step is the determination of the equilibrium value of S_0 derived from the condition $dF/dS_0=0$ and is given by the following expression:

$$S_0=\frac{G}{2a(T-T^*)\xi[\tanh(R/\xi)-(\xi/2R)\tanh^2(R/\xi)+(\xi^2/R^2)\cosh^{-2}(R/\xi)]} . \tag{8}$$

In the limit $R \gg \xi$, Eq. (8) simplifies to the following form:

$$S_0=\frac{G}{[4aL(T-T^*)]^{1/2}}=S_{00}\frac{1}{2(T/T^*-1)]^{1/2}} , \tag{9}$$

where $S_{00}=G/(aLT^*)^{1/2}$. The minimization process yields a description of the profile of nematic orientational order as a function of distance from the cavity wall [Eqs. (4) and (7)], and identifies the order parameter at the surface of the cavity wall [Eqs. (8) and (9)].

Actually, the cross sections of the sample pores are not circular, but represent irregularly shaped hexagons (Fig. 1). However, as long as the correlation length of the ordered material is small compared to the pore size R, Eqs. (7) and (9) remain valid if R is assigned an average half-distance value between opposite sides of the pores.

III. MEASUREMENT OF THE SURFACE ORDER PARAMETER VIA ^{2}H-NMR

^{2}H-NMR provides a direct measure of the orientational order at the molecular level via the time-averaged quadrupole-splitting frequency from a selectively deuterated liquid-crystal molecule [18]. We consider a molecule at a local position of the cavity to be represented by the position vector $\mathbf{r}$. In the absence of motional averaging, a compound deuterated at a specific site will yield a spectrum of two sharp lines separated by

$$\delta\nu(\mathbf{r})=\frac{S(r)}{S_B}\delta\nu_B[\tfrac{3}{2}\cos^2\theta(\mathbf{r})-\tfrac{1}{2}] , \tag{10}$$

where $\theta(\mathbf{r})$ is the angle between the local nematic director and the magnetic field, $S(\mathbf{r})$ the local order parameter given by Eq. (7), and $\delta\nu_B/S_B$ the ratio between the quadrupole-splitting frequency and the order parameter of the bulk nematic. In the isotropic phase far from the surface of the cavity wall, the order parameter $S(\mathbf{r})$ is zero and the quadrupolar interactions are completely averaged to zero. The systems employed in this investigation exhibit a large surface-to-volume ratio giving rise to a definite quadrupole splitting above the N-I transition as a result of surface-induced nematic order. The important characteristics of the ^{2}H-NMR line shapes in our studies conducted in the isotropic phase depend on three factors: the anchoring conditions of the molecule at the surface, the orientation of the pore axis with respect to the magnetic field, and the extent of translational self-diffusion. Since the resonance frequency depends on the angle between the nematic director and the external field as seen from Eq. (10), the ^{2}H-NMR spectral pattern is a direct indication of the orientational arrangement of the molecules inside the cavity.

The surface of the cavity competes with the magnetic field of the NMR spectrometer in aligning the directors. The influence of this field can be estimated by the magnetic coherence length ξ_m given by

$$\xi_m=\left[\frac{\mu_o K}{\Delta_X}\right]^{1/2}\frac{1}{B} , \tag{11}$$

where K is a combination of elastic constants and Δ_X is the anisotropy of the diamagnetic susceptibility. The strength of the magnetic field in our experiments is $B=4.7$ T, corresponding to a magnetic coherence length of $\xi_m \sim 1.7$ μm (for 5CB) [19], which is substantially larger than the diameters of the cavities used. In particular, it exceeds the thickness of the surface-induced nematic order by several orders of magnitude. Therefore, the magnetic field does not introduce any measurable distortion of the director field and can be neglected.

In the temperature range above the N-I transition where the correlation length of the nematic order is small, the radial dependence of θ can be neglected. The thickness of the ordered interfacial layer is small compared to the curvature of the cavity walls and can also assume that θ depends only upon the director orientation at the surface. As will be shown below, fast motional averaging at temperatures above the N-I transition makes it impossible to determine the anchoring angle from the angular dependence of the spectral patterns. In order to determine the anchoring angle, ^{2}H-NMR spectra were recorded in the nematic phase. We assume that the orientation of the nematic director in the nematic phase is identical to that of the ordered surface layer in the isotropic phase. We have considered three principal orientations of the director at the cavity wall: Parallel axial alignment at the surface along the cylinder axis as depicted in Fig. 2(a), parallel tangential alignment as shown in Fig. 2(b), and perpendicular radial alignment as shown in Fig. 2(c). Figure 2(a) defines θ_H to be that angle between the cylinder axis and the magnetic field. For parallel axial alignment, θ is equal to θ_H. For the parallel tangential orientation, the angle θ between the magnetic field and the director is given by $\cos\theta=\sin\theta_H \sin\Phi$, and for the perpendicular radial alignment $\cos\theta=\sin\theta_H \cos\Phi$, where Φ is the azimuthal angle defined in Fig. 2. These director configurations can easily be identified by the ^{2}H-NMR spectra in the nematic phase, as will be shown later.

Translational diffusion in the isotropic phase leads to a fast exchange of the molecular positions during the NMR measurement. The average displacement x_0 of a mole-

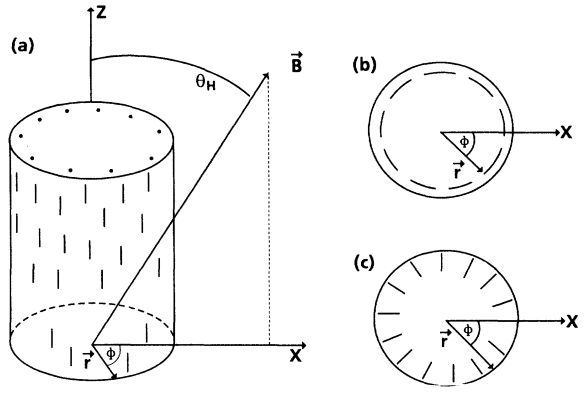

FIG. 2. Schematic illustration of the geometry and angles defined in the text: (a) the case of parallel axial anchoring at a surface parallel to the cylinder axis, (b) parallel tangential anchoring at a surface perpendicular to the cylinder axis, and (c) radial anchoring at a surface perpendicular to the cylinder axis.

cule due to diffusion during a time t is of the order $x_0 \sim \sqrt{Dt}$. The length of the free induction decay (FID), which is the measurement time, is of the order of 1.0 ms, and the diffusion constant $D \sim 10^{-10}$ m^2/s in the isotropic phase, the distance the molecule migrates is larger than the pore diameter. The quadrupole-splitting frequency given in Eq. (10) is thus completely averaged to the same value $\langle \delta\nu \rangle$ for all spins in the sample where $\langle\ \rangle$ denote spatial averaging. According to Eq. (10), the resonance frequencies are linear dependent upon the order parameter, but the radial and tangential motions are not correlated. Therefore we can perform the averaging of $S(r)$ and $\theta(\Phi)$ separately, i.e., each molecule experiences an average order parameter $\langle S \rangle$ which results in a reduced quadrupole-splitting frequency. The angle Φ is randomly distributed in the sample, resulting in $\langle \cos^2\Phi \rangle = \langle \sin^2\Phi \rangle = \frac{1}{2}$. Therefore, the angular dependence of Eq. (10) is averaged to

$$\langle \delta\nu \rangle \propto \langle \tfrac{3}{2}\cos^2\theta - \tfrac{1}{2} \rangle \propto \tfrac{3}{2}\cos^2\theta_H - \tfrac{1}{2} \tag{12}$$

for all configurations considered. In the isotropic phase, the molecular alignment of the surface-induced nematic order is not attainable at the cavity wall, and one must resort to the nematic phase for this information described earlier.

For cylindrical symmetry, the average order parameter can be calculated by the following expression:

$$\langle S \rangle = \langle S(r) \rangle = \frac{\int_0^R S(r) r\, dr}{\int_0^R r\, dr} , \tag{13}$$

which is directly proportional to the time-averaged quadrupole splitting given by the following relation:

$$\langle \delta\nu \rangle = \frac{\delta\nu_B}{S_B} \langle S \rangle \left| \tfrac{3}{2}\cos^2\theta_H - \tfrac{1}{2} \right| . \tag{14}$$

The function $S(r)$ expressed in Eq. (7) can be substituted into Eq. (13) to obtain the analytical expression for the average order parameter given by the expression

$$\langle S \rangle = \frac{2S_0\xi}{R} = \frac{G}{aR(T - T^*)} , \tag{15}$$

where ξ and S_0 are described by Eqs. (5) and (9), respectively. Substitution of Eq. (15) into Eq. (14) establishes a relation to describe the temperature dependence of the measured quadrupole-splitting frequency of a ^{2}H-NMR measurement.

The theory presented above does not provide an adequate description of orientational wetting phenomena in our experimental systems. It leads to a much faster decrease of the quadrupole-splitting frequency with increasing temperature than our experiments show. For a better description of the experimental data, an interfacial surface-layer model is employed that was previously used to describe orientational ordering phenomena of a liquid crystal confined to the submicrometer cylindrical cavities of polymeric Nuclepore membranes [14]. The profile of the surface-induced nematic order given by Eq. (7) can now be expressed in modified form as

$$S(r) = \begin{cases} S_0, & R \le r \le R - l_0 \\ S_0 e^{-[(R-l_0)-r]/\xi}, & R - l_0 \le r \le 0 \end{cases} \tag{16}$$

where l_0 is the interfacial thickness of the surface layer, approximately on the order of molecular dimensions. Such behavior can be expected when the interactions of the liquid-crystal molecules with the cavity wall is local in nature. The order-parameter profile of Eq. (16) is presented in Fig. 3 for various values of R/ξ, where the inset clearly illustrates the interfacial surface layer. Upon substitution of Eq. (16) into Eq. (13) and performing the integration in the limit $l_0 \ll R$, the average order parameter can be derived in close form described by the analytical expression

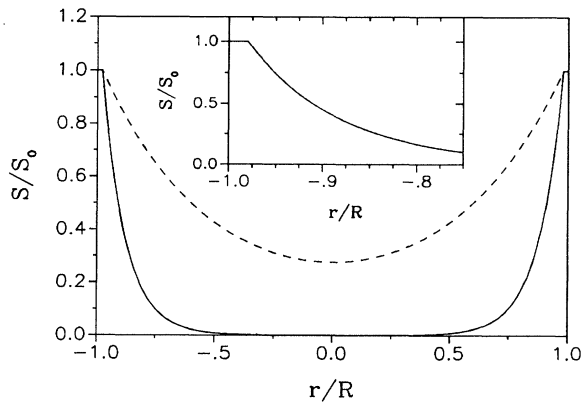

FIG. 3. The molecular orientational order-parameter profile in a cylindrical environment. The solid curve is calculated for $R/\xi = 10$, the dashed curve is calculated for $R/\xi = 2$, and the inset illustrates the interfacial layer at the cylinder wall needed to explain order observed at temperatures far above $T_{N\text{-}I}$.

$$\langle S \rangle = \frac{2S_0\xi}{R} + \frac{2S_0 l_0}{R} , \quad (17)$$

where $\xi = \xi(T)$ is assumed to behave according to Landau–de Gennes predictions expressed by Eq. (5), and S_0 can be described by Eq. (9) or, in some experimental systems, as temperature independent [14]. Equation (17) consists of two terms which describe the bulk contribution ($2S_0\xi/R$) and the interfacial layer contribution ($2S_0 l_0/R$) to the molecular order parameter. The bulk contribution dominates near the N-I transition because the correlation length ξ is large, but deep in the isotropic phase ($T - T_{N\text{-}I} \sim 15$ K) the interfacial layer term becomes the dominant contribution to the ^{2}H-NMR quadrupole-splitting frequency. We have assumed to the first approximation that l_0 is temperature independent.

IV. EXPERIMENTAL METHOD AND SAMPLE PREPARATION

For surfaces to be accessible with ^{2}H-NMR, a system with a large surface-to-volume ratio must be realized. The pores in Anopore inorganic membranes [20] (see Fig. 1) are filled with a liquid-crystalline material exhibiting these properties and provide an ideal system by which to investigate molecular interactions with solid surfaces. The channels of the membranes are "honeycomb"-shaped regular capillary pores with an extremely narrow pore-size distribution. The membrane is composed of a high-purity alumina matrix with 0.2-μm diam channels oriented perpendicular to the membrane surface and penetrating through its 60-μm thickness [21]. The membranes were sliced into 4-mm-wide strips, 25 mm in length. They were wetted with a small amount of nematic material. The wetted membranes were taken above the N-I transition temperature for approximately 1 h to ensure complete wetting of the channels. The excess liquid crystal on the top surface of the membrane was completely removed by pressing them between Walthan filtration papers. Forty strips were uniformly stacked and placed in a 5-mm Norell precision thin-walled NMR tube.

The Anopore membranes are produced by Anotec Separations from an electrochemical anodizing process and generally used for critical filtration applications [21]. They are chemically compatible with many solvents, allowing the surface to be treated with different surfactants or polymers. Lecithin and poly(isobutyl methacrylate) (PIBMA) were used in our experiments to systematically treat the surface. A 1.5%-by-weight solution of lecithin (Sigma Chemical Company) in hexane was prepared and capillary-filled into the membrane and then placed in a vacuum oven for several hours to ensure the complete removal of the solvent. Lecithin is a surfactant widely used for homeotropic surface alignment of nematic liquid crystals. Another surface treatment was achieved by preparing a 1.5%-by-weight solution of PIBMA (Aldrich Chemical Company, Inc.) in chloroform. This polymer was shown to give perpendicular boundary conditions in polymer-dispersed liquid-crystal droplets [22].

The liquid-crystal material used in this surface-order study was 5CB-βd_2 (4-n-pentyl-4′-cyanobiphenyl) deuterated in the second position from the aromatic rings on the hydrocarbon chain. The purity of the 5CB-βd_2 is 99.6% as determined by high-pressure liquid chromatography (HPLC) [23]. Another liquid crystal was used consisting of a 20%-by-weight mixture of 4-n-methoxy-4′-cyanobiphenyl (10CB-d_3) deuterated in the methyl position with protonated 5CB.

The experiments were performed on a home-built coherent-pulse solid-state spectrometer with a 4.7-T magnetic field designed primarily for orientational and phase transition studies of liquid crystals. A modified quadrupolar echo sequence $(\pi/2)_x$-τ-$(\pi/2)_y$ was employed where $\tau = 100$ μs and the length of the $\pi/2$ pulse was 5 μs. The FID was averaged 2000 times to achieve a reasonable signal-to-noise ratio. The temperature is regulated by a circulating fluid bath with resolution of 0.1 °C and stability in the sample of 0.05 °C. The temperature is directly recorded from the sample chamber. The orientation of the sample about the axis perpendicular to the magnetic field can be varied by a stepper motor with 0.05° resolution in θ_0. The sample is stacked in the NMR tube such that the cylinder axes of the channels are parallel to the magnetic field, and can be rotated through 90° such that the cylinder axis are perpendicular to the magnetic field. This allows the profile of the nematic order in the cavity to be projected in different directions.

The quadrupolar coupling constant was calculated using the value $\nu_q = eQV_{zz}/h = 175$ kHz for the interaction between the electric-field-gradient tensor V and the quadrupole moment of the chain deuteron in a rigid molecule, where z is the direction of the carbon-deuterium bond and eQ is the nuclear quadrupole moment. Considering the bond angles in the 5CB molecule and assuming the long molecular axis parallel to the benzene-ring para axis, the ratio $\delta\nu_B/S_B$ in the nematic phase is 87.5 kHz. In the 10CB molecules, the quadrupolar coupling of the methyl deuterons is additionally averaged by the fast rotations of the CD_3 group, and the ratio $\delta\nu_B/S_B$ is about one order of magnitude smaller.

V. EXPERIMENTAL RESULTS AND DISCUSSION

A. Nematic phase

A liquid crystal confined to a cylindrical-type environment in the nematic phase exhibits a specific director configuration resulting from an interplay between elastic forces, the effect of the magnetic field, morphology and size of cavity, and surface interactions. The specific functional form of the nematic director configuration can be derived from elastic theory and has been considered elsewhere for confined systems [24–27]. Motional averaging has a minimal effect in the nematic phase, resulting in the ^{2}H-NMR spectral pattern reflecting the static distribution of directors in the cavity, and the order parameter can be taken as constant throughout the volume of the cylinder $S(\mathbf{r}) = S = \text{const}$. These characteristics allow the distribution of molecular alignment to be determined in the nematic phase. It can be seen from Eq. (10) that the resonance frequency depends on the orientation of the magnetic field in the director frame (principal-axis frame)

of the phase. In the case of macroscopically aligned samples, only two absorption lines are expected, which is characteristic of a bulk nematic phase aligned by the magnetic field. For the case where the directors are not uniformly aligned in the magnetic field, a spectral powder pattern will result that is a direct indication of the director distribution.

We have determined the director distributions in our systems for treated and untreated cavities. Two orientations of the cylinder axis in the magnetic field were investigated ($\theta_H=0°$ and 90°) to project the profile of the configuration in different directions. For the untreated cavities presented in Fig. 4(a), the $\theta_H=0^{\circ}$ orientation yields two singularities separated by $\delta\nu=(\delta\nu_B/S_B)S$, which corresponds to the contribution of molecules with the director frame oriented at an angle $\theta=0°$. For the $\theta_H=90°$ orientation, the two singularities are separated by $\delta\nu=\frac{1}{2}(\delta\nu_B/S_B)S$, corresponding to the contributions of molecules with their director frame oriented at an angle $\theta=90°$. A more detailed study of this sample yields the classical $P_2(\cos\theta_H)$ dependence, confirming the alignment to be parallel axial as illustrated in Fig. 2(a). For the lecithin-treated cylinder presented in Fig. 4(b), the $\theta_H=0°$ orientation yields two singularities separated by $\delta\nu=\frac{1}{2}(\delta\nu_B/S_B)S$, indicating that the directors are oriented at an angle $\theta=90°$. When the cylinder axis is oriented perpendicular to the magnetic field $\theta_H=90°$, the angle θ is uniformly distributed in a cylindrical distribution, resulting in a classical cylindrical powder pattern [28]. The molecular alignment in this lecithin-treated cavity is perpendicular radial alignment shown in Fig. 2(b). The PIBMA-treated surface presented in Fig. 4(c) is identical to the spectra in Fig. 4(a), indicating the parallel axial alignment. This contradicts the observation of radial anchoring conditions in polymer-dispersed liquid-crystal droplets [22] and will be discussed later.

B. Isotropic phase

Experimental ^{2}H-NMR spectra for 5CB-βd_2 in untreated and lecithin-treated cavities at various angles in the magnetic-field are presented in Fig. 5. If we consider a truly isotropic sample, there is no quadrupole interaction resulting in a single absorption line of width $\sim$30 Hz (linewidth governed by field inhomogeneity) invariant to the angle in the magnetic field. The presence of the quadrupole interaction is responsible for the spectral splitting frequency $\delta\nu$ and the angular dependence shown in Fig. 5. This clearly identifies the presence of surface-induced nematic order in the isotropic phase in these confined systems. The complete angular dependence for the untreated and lecithin-treated cavities is shown in Fig. 6, where the solid curve is the theoretical fit to Eq. (12). The quadrupole splittings close to the magic angle coalesce into a single line and are unresolvable. The untreated (parallel alignment) and lecithin-treated (perpendicular alignment) both follow the same angular dependence given by Eq.

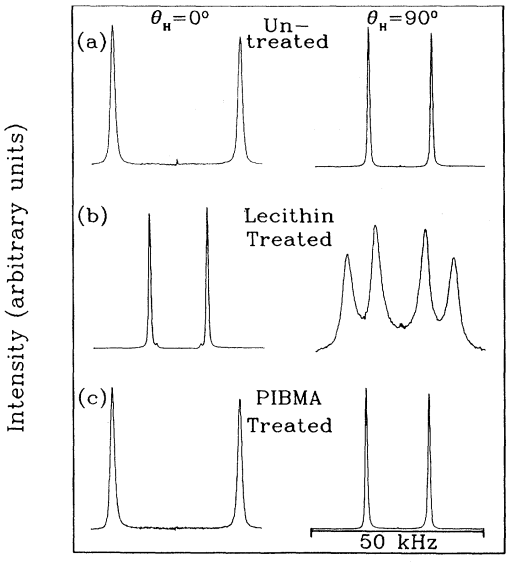

FIG. 4. Experimental ^{2}H-NMR spectra recorded deep in the nematic phase for channel axes parallel ($\theta_H=0°$) and perpendicular ($\theta_H=90°$) to the magnetic field for 5CB-βd_2 confined in Anopore membranes for (a) the untreated, (b) lecithin-treated, and (c) PIBMA-treated cavities.

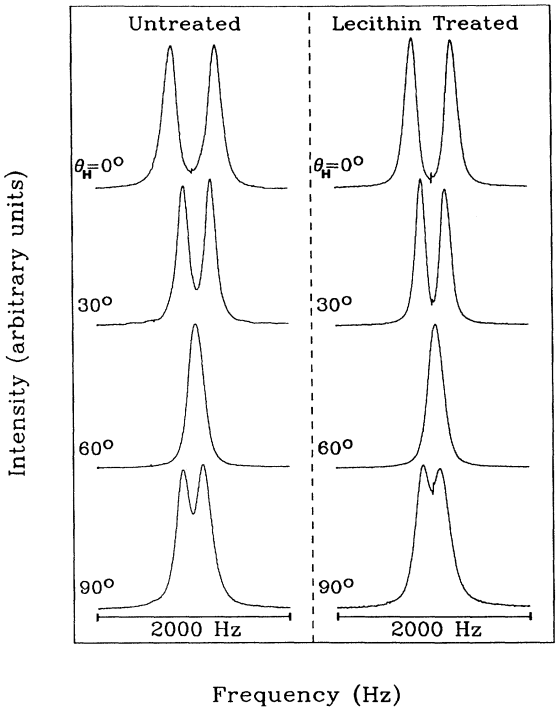

FIG. 5. Experimental ^{2}H-NMR spectra for 5CB-βd_2 in Anopore membranes in the isotropic phase for various angles of the channel axis in the magnetic field for the untreated case recorded at $T-T_{N\text{-}I}=0.5$ K and lecithin-treated cavities recorded at $T-T_{N\text{-}I}=2.3$ K.

(12), confirming our statement that we are in the fast-motional-averaging regime. In addition, the liquid-crystal material 10CB-d_3 was investigated in untreated cavities. This system is additionally averaged because of the rapid motions of the CD_3 group resulting in only one absorption line of width 123 Hz. This is substantially broader than the isotropic line, indicting that there exists a small quadrupole splitting which is expected and is unresolvable in our spectrometer.

Experimental ^{2}H-NMR spectra for 5CB-βd_2 confined to untreated and lecithin-treated cavities is presented in Fig. 7. As the N-I transition is approached, the quadrupole-splitting frequency increases as a direct consequence of the critical behavior of the correlation length predicted by Eq. (5). It is apparent from these spectra that a definite quadrupole splitting exists deep in the isotropic phase for both cases. This is not predicted by existing theories as can be seen in Fig. 8. The quadrupole splitting of the 5CB-βd_2-untreated system is plotted as a function of reduced temperature, where the curves represent the theoretical model expressed by Eq. (15). The theoretical curves are plotted for values of $\xi_0=6.5$ Å and $T^*=307$ K for $S_{00}=2.5\times10^{-3}$ (solid curve) and

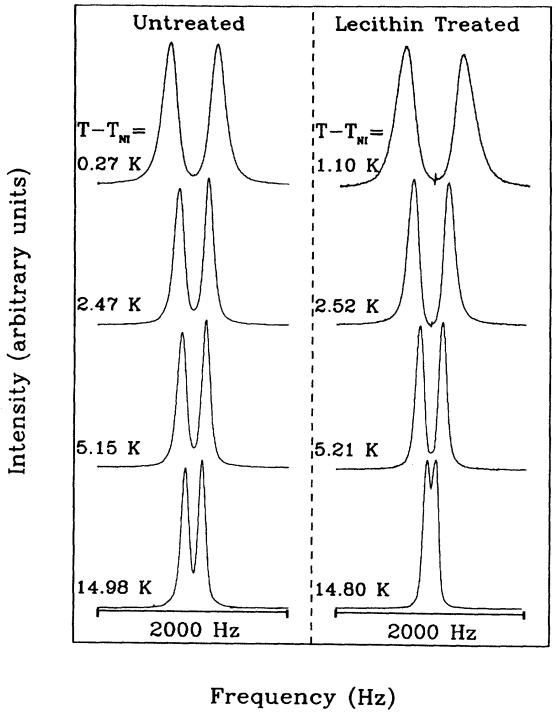

FIG. 7. Experimental ^{2}H-NMR spectra for 5CB-βd_2 in Anopore membranes recorded at various temperatures in the isotropic phase for the untreated and lecithin treated cavities. The channel axes are oriented parallel to the magnetic field.

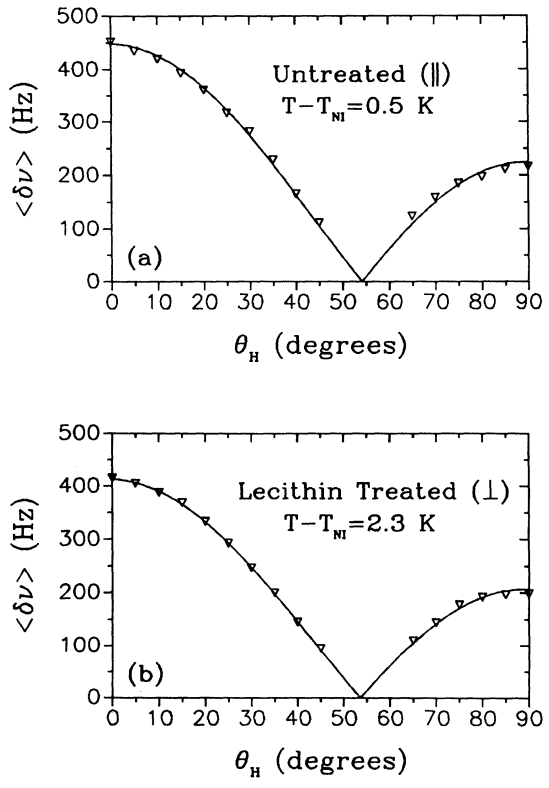

FIG. 6. Angular dependence of the quadrupole splitting for 5CB-βd_2 in Anopore membranes recorded in the isotropic phase for (a) the untreated cavities with parallel axial alignment and (b) lecithin-treated cavities with perpendicular radial alignment. The solid curve is the theoretical fit predicted by Eq. (12).

$S_{00}=7.5\times10^{-3}$ (dashed curve). It is evident from Fig. 8 that a good fit near the N-I transition (solid curve) results in a faster decrease of the quadrupole splitting than our data show. If the data are fitted deep in the isotropic phase (dashed curve), then it fails to predict the critical phenomena near the N-I transition. This was the same behavior exhibited by Nuclepore systems whose submicrometer cylindrical cavities were filled with 5CB-βd_2 [14]. Therefore, the theory was modified to include an additional temperature-independent interfacial surface layer shown in Fig. 3 and expressed by Eqs. (16) and (17).

Additional evidence for a different behavior of the first molecular layer can be seen by experimentally deriving the order parameter at the cavity wall as a function of temperature using the well-accepted Landau–de Gennes bulk form $\langle S\rangle=2S_0\xi/R$, where ξ is described by Eq. (5). The results are presented in Fig. 8(b) for $T_{N\text{-}I}-T^*=1.1$ K and $\xi_0=6.5$ Å [29]. The value of S_0 increases slightly as a function of temperature, which is an unphysical trend. An explanation for this behavior can be understood by examining Eq. (5) as $T\rightarrow2T^*$, resulting in $\xi\rightarrow\xi_0=6.5$ Å, which is substantially smaller than one molecular length. This does not incorporate the dominant ordering interactions experienced by the molecules near the cavity wall. Inclusion of an additional ordered surface layer results in a noncritical, in the first approximation, temperature-independent surface order parameter, shown in Fig. 8(c).

The temperature dependence of the measured

quadrupole-splitting frequency is presented in Fig. 9 for three different surfaces whose channel axes are parallel to the magnetic field ($\theta_H = 0°$). We will assume the form of the $\frac{1}{2}$ power law of the correlation length given by Eq. (5),

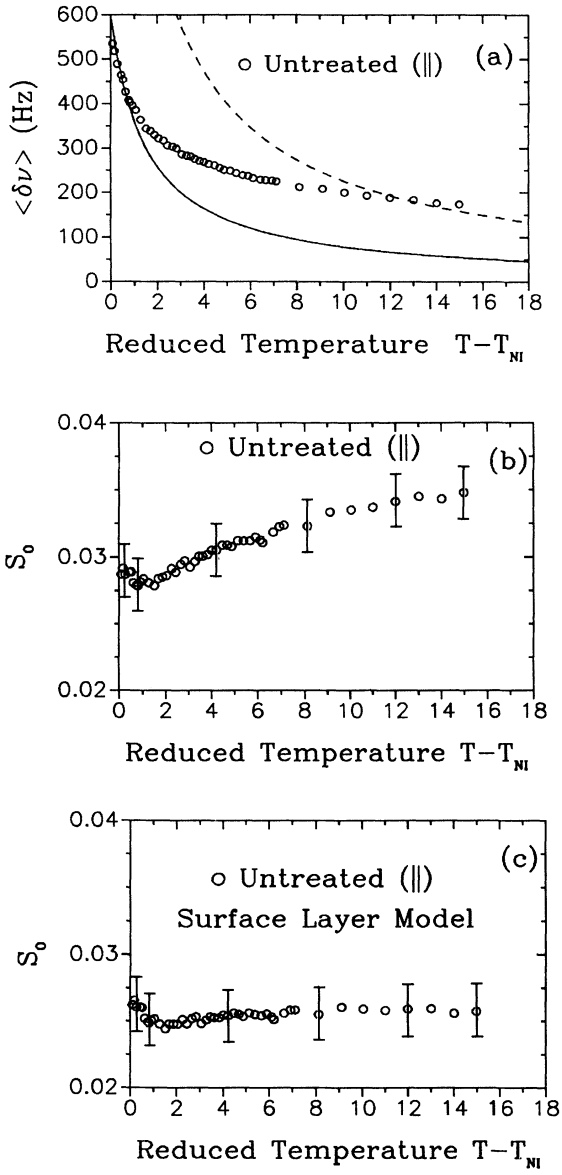

FIG. 8. Temperature dependence of the quadrupole-splitting frequency $\langle \delta\nu \rangle$ and surface order parameter S_0 in the isotropic phase for 5CB-βd_2 confined in untreated Anopore membranes, where $\xi_0 = 6.5$ Å and $T_{N\text{-}I} - T^* = 1.1$ K are used in the calculations. (a) Theoretical curves for $S_{00} = 2.5 \times 10^{-3}$ (solid curve) and $S_{00} = 7.5 \times 10^{-3}$ (dashed curve) using Eqs. (14) and (15) demonstrating an inadequate description of the orientational order present deep in the isotropic phase. (b) The order parameter at the cavity wall derived experimentally using $\langle S \rangle = 2S_0\xi/R$ yielding an unphysical behavior of S_0, and (c) the inclusion of the ordered surface layer expressed by Eq. (17) with $l_0 = 10$ Å yielding a noncritical, temperature-independent S_0.

which is well established in the literature, but we will consider two forms of the surface order parameter. First, we consider a temperature-dependent surface order parameter expressed by Eq. (9). Employing the profile of the order parameter in its modified form Eq. (16), the temperature dependence of the quadrupole-splitting frequency can be derived by substitution of Eq. (17) into Eq. (14), yielding the expression

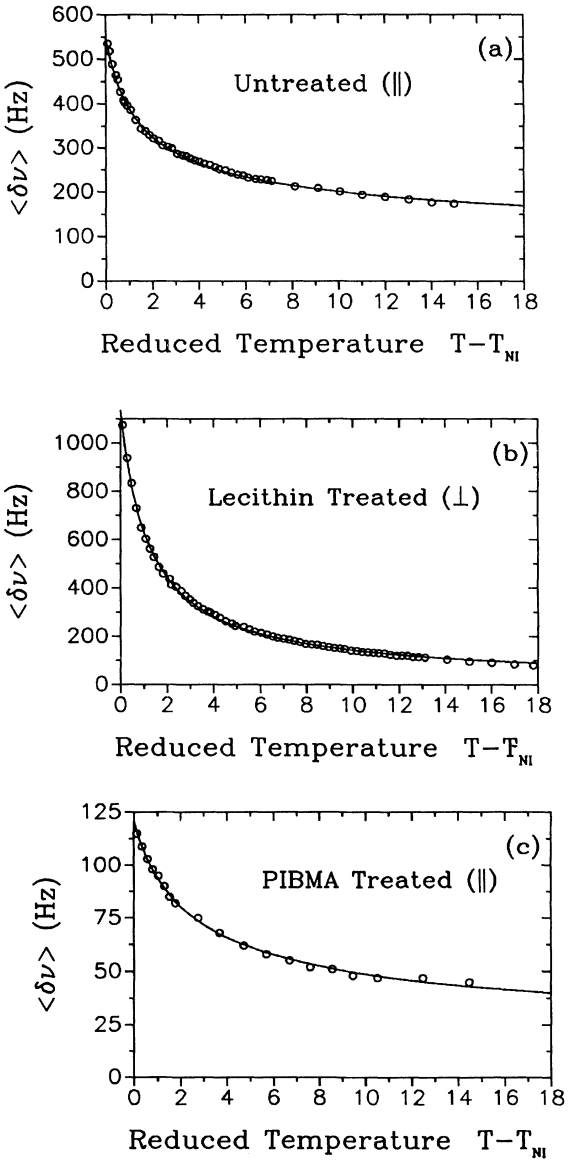

FIG. 9. Temperature dependence of the quadrupole-splitting frequency for 5CB-βd_2 in Anopore membranes with the channel axis parallel to the magnetic field for (a) the untreated, (b) lecithin-treated, and (c) PIBMA-treated cavities. The solid curves represent the theoretical fits to the temperature-independent S_0 model, (a) and (c), expressed by Eq. (19) and the temperature-dependent S_0 model, (b), expressed by Eq. (18).

$$\langle \delta v \rangle = \frac{\delta v_B}{S_B} \left[\frac{A}{(T-T^*)} + \frac{B}{(T-T^*)^{1/2}} \right], \quad (18)$$

where the angular dependence term is $\frac{1}{2}(3\cos^2\theta_H - 1) = 1$ since $\theta_H = 0°$, $A = 2\xi_0 S_{00} T^*/R$, $B = 2l_0 S_{00}(T^*)^{1/2}/R$, and $S_{00} = G/(aLT^*)^{1/2}$. This is a three-parameter function, where A, B, and T^* are the fitting parameters. A and B are quantities with units K and $K^{1/2}$, respectively, used to determine S_0 and l_0.

Assuming the surface order parameter to be independent of temperature [14], the temperature dependence of $\langle \delta v \rangle$ becomes

$$\langle \delta v \rangle = \frac{\delta v_B}{S_B} \left[\frac{A'}{(T-T^*)^{1/2}} + B' \right], \quad (19)$$

where $A' = 2\xi_0 S_0 (T^*)^{1/2}/R$ and $B' = 2l_0 S_0/R$. Again, this is a three-parameter model where A', B', and T^* are fitting parameters used in the determination of S_0 and l_0. In this model the fitted parameters A' and B' are quantities with units $K^{1/2}$ and dimensionless, respectively. A temperature-independent S_0 is not predicted by the Sheng theory [2], but has been experimentally observed in Nuclepore systems [14].

We have used the models presented in Eqs. (18) and (19) to analyze our experimental data. For the untreated cavities in Fig. 9(a), the best fit was obtained using the temperature-independent surface order-parameter model given by Eq. (19), where $S_0 = 0.021 \pm 0.002$, $l_0 = 19.3 \pm 2.0$ Å, and $T_{N\text{-}I} - T^* = 0.87 \pm 0.05$ K using the value $\xi_0 = 6.5$ Å reported in the literature [29]. The value of l_0 may seem large for parallel alignment at the surface, but the quadrupole interaction deep in the isotropic phase ($T_{N\text{-}I} - T \sim 15$ K) remains extremely large ($\langle \delta v \rangle \approx 175$ Hz), indicating an ordered layer at the surface which has a weak temperature dependence. For the lecithin-treated cavities in Fig. 9(b), the best fit was obtained using the temperature-dependent order-parameter model described by Eq. (18), where $S_{00} = 0.007 \pm 0.001$, $l_0 = 11.4 \pm 2.0$ Å, and $T_{N\text{-}I} - T^* = 1.16 \pm 0.05$ K. The value measured for S_{00} yields values for the surface order parameter near the N-I transition $S_0(T - T_{N\text{-}I} = 0.08\ \text{K}) = 0.110 \pm 0.002$ and deep in the isotropic phase $S_0(T - T_{N\text{-}I} = 17.90\ \text{K}) = 0.028 \pm 0.002$, similar to the value for the untreated cavity. The temperature dependence of the PIBMA-treated cavities was best fitted to the temperature-independent surface order-parameter model given by Eq. (19). The fitting parameters were determined to be $S_0 = 0.006 \pm 0.002$, $l_0 = 10.3 \pm 2.0$ Å, and $T_{N\text{-}I} - T^* = 1.20 \pm 0.05$ K. The values of $T_{N\text{-}I} - T^*$ for all three systems agree well with the predicted value of $T^* - T_{N\text{-}I} = 2B^2/9aC = 1.1$ K from the Landau–de Gennes formalism [16]. The summary of the fitting parameters for various surface treatments is presented in Table I. The experimental interfacial surface parameters determined by fitting the data in Fig. 9 to Eqs. (18) and (19) is summarized in Table II. Comparing the experimental data in Figs. 9(a) and 9(b) far away from the N-I transition, the untreated cavity in Fig. 9(a) has a quadrupole-splitting frequency twice as large as the lecithin-treated cavities in Fig. 9(b). At these temperatures the splitting is principally governed by the order of the first molecular layer in both systems, so the difference in the quadrupole splitting is attributed to the factor of 2 that distinguishes parallel and perpendicular orientations of the long molecular axis in the magnetic field given by Eq. (10).

There have been several other measurements of the surface order parameter on various interfaces. Most recently, the cylindrical polymer cavities of Nuclepore membranes were filled with 5CB-βd_2 to investigate ordering and diffusion at the surface [14]. Employing various cylinder sizes, the quadrupole splitting was shown to increase in decreasing cylinder sizes because of increased surface-to-volume ratio. By simultaneously fitting ^{2}H-NMR spectra of different cavity sizes with the same fitting parameters, the surface order parameter was determined to be $S_0 = 0.02$ for the entire temperature range studied. This value and the behavior of the temperature dependence is similar to the untreated and PIBMA-treated cavities with a weak S_0 that is temperature independent. Barbero and Durand [11] have measured S_0 to be in the range $S_0 \sim 0.1$–0.25, depending on the roughness induced by oblique evaporation of SiO. Chen

TABLE I. Fitting parameters determined from data in Fig. 9 for the temperature-independent S_0 model expressed by Eq. (19) and temperature-dependent S_0 model expressed by Eq. (18) for 5CB-βd_2 confined in Anopore membranes for various surface treatments.

		Temperature-independent S_0 model		
Surface	Alignment (nematic phase)	$A'(K^{1/2}$ (units of $10^{-3})$	B' (units of 10^{-3})	$T^*(°C)$
Untreated	Parallel axial	4.83±0.05	0.81±0.05	34.23±0.03
PIBMA treated	Parallel axial	1.43±0.05	0.13±0.05	32.69±0.03
		Temperature-dependent S_0 model		
Surface	Alignment (nematic phase)	$A(K)$ (units of 10^{-3})	$B(K^{1/2})$ (units of 10^{-3})	T^* (°C)
Lecithin-treated	Radial perpendicular	27.17±0.05	2.74±0.05	29.64±0.03

TABLE II. Summary of interfacial surface parameters for 5CB-βd_2 confined in Anopore membranes with various surface treatments.

Temperature-independent S_0 model					
Surface	Alignment (nematic phase)	S_0	l_0 (Å)	$T_{N\text{-}I}-T^*$ (K)	G (10^{-5} J/m^2)
Untreated	Parallel axial	0.021±0.002	19.3±2.0	0.87±0.05	≤ 5.9[a]
PIBMA-treated	Parallel axial	0.006±0.002	10.3±2.0	1.2±0.05	≤ 2.0[a]
Temperature-dependent S_0 model					
Surface	Alignment (nematic phase)	S_{00}	l_0 (Å)	$T_{N\text{-}I}-T^*$ (K)	G (10^{-5} J/m^2)
Lecithin-treated	Radial perpendicular	0.007±0.001	11.4±2.0	1.16±0.05	37±1.0

[a]Estimate of upper boundary.

et al. [9] have measured S_0 for 5CB at a silane-treated glass substrate to be $S_0 \sim 0.2$, with only a weak temperature dependence near the N-I transition. Yokoyama *et al.* [12] have reported values as small as $S_0 \sim 0.01$ for a 5CB-SiO interface. The difference in values of S_0 can be attributed to the different surface treatments used resulting in a different substrate-fluid interaction.

The measurement of the surface order parameter is a direct measure of the strength of the substrate-fluid interaction, which is often called the surface coupling constant. By treating the surface we have effectively changed this surface coupling constant G, which is related to the surface order parameter S_0 in Eq. (9). For the temperature-independent S_0 model, we can only estimate the upper limit of G using the relation $G \leq S_0[4aL(T_{N\text{-}I}-T^*)]^{1/2}$. The material constants for 5CB are the elastic constant $L = 1.7\times10^{-11}$ J/m and the Landau–de Gennes expansion coefficient $a = 0.1319\times10^6$ J/m^3 K [29]. The upper-bound values of G for the untreated and PIBMA-treated cavities are 5.9×10^{-5} and 2.0×10^{-5} J/m^2, respectively. These values are of the same order of magnitude that were reported for the 5CB-βd_2–polymer surface in Nuclepore cavities [14]. The small values of S_0 in these systems governs this weak surface coupling to the orientational order parameter of Sheng's type. Our estimates of G for the temperature-independent S_0 model are much smaller than the value 4.0×10^{-4} J/m^2 needed for the existence of the prewetting transition which was not observed here or elsewhere. For the temperature-dependent S_0 model used in the fitting process of the lecithin-treated cavities, the surface coupling constant can be determined accurately from Eq. (9) to be 3.7×10^{-4} J/m^2. This value is only slightly less than the lower limit predicted by Sheng for the prewetting transition to occur. There was also no evidence of a prewetting transition in these lecithin-treated cavities. The values of G are also summarized in Table II.

Although the quadrupole interaction is present in our systems above the N-I transition, the N-I transition is still characterized by a discontinuity in the quadrupole-splitting frequency of more than one order of magnitude. At the N-I transition both the nematic and surface-induced nematic signals are observed indicating a first-order phase transition. Since the cavity sizes employed in this study are 0.2 μm in diameter, it is well above the critical size needed for the N-I transition to change to a continual evolution from paranematic to nematic order [30].

As seen from Tables I and II, there is a temperature depression of the transition temperature which does not affect the critical behavior of the correlation length, but slightly rescales the temperature, and thus only results in small changes in the material constants. There are two competing mechanisms which can shift the transition temperature: surface-induced order which tends to increase the transition temperature [2], and geometry-introduced elastic deformation, which tends to decrease the transition temperature. Only the latter effect can describe the depression in T^* which is of the order L/R^2a, which is much less than 1 for $R \sim 0.1$ μm. Therefore, we attribute this behavior to impurities introduced from the surface treatment used and, to a much lesser extent, the elastic deformation introduced by the confining walls. Our approach here is to describe the exciting physics of surface-induced nematic ordering, both the pretransition and interfacial surface layer effects for various treatments of the cavity walls in these systems.

VI. CONCLUSIONS

The data reported here clearly show surface-induced molecular ordering at temperatures deep in the isotropic phase which cannot be explained by Landau–de Gennes theory. This residual order was not reported by earlier investigators, perhaps because their data were taken at temperatures very near $T_{N\text{-}I}$ where the Landau–de Gennes equations are dominant. We find that this observed residual order at high temperatures can be well explained by the order of the first molecular layer only. This order is present at elevated temperatures because it is governed by local interactions between the first layer and the cavity wall. These interactions, being molecular in nature, are weakly temperature dependent.

The degree of order S_0 of this layer was measured for three different surface preparations and found to be significantly affected by them. Untreated surfaces of the Anopore cavities and treatment by the polymer PIBMA

both yielded a weak surface coupling constant G with values of S_0 showing no measurable temperature dependence over the 15-°C range studied. The surface treated with lecithin showed an order-of-magnitude-larger value for surface coupling constant G, and a value of S_0 which varied in temperature, as expected from the Sheng theory, which incorporates constants of such a magnitude. The large value of G measured for the lecithin system was not, however, large enough to expect the presence of the surface layer transition (prewetting transition) predicted by Sheng and is perhaps the reason this transition has never been observed. It may be possible to describe the temperature dependence and interfacial surface layer behavior by including nonlinear terms in the free-energy density and quadratic surface terms [31].

It is also the subject of future study to look for surface treatments that exhibit extreme values of the surface coupling strength. A strong value of the surface coupling constant may reveal the existence of a prewetting transition. For weak surface coupling as exhibited by the PIBMA-treated cavities, the competition between the elastic energies and the finite anchoring energies in the nematic phase could provide valuable insight into the development of liquid-crystal-based devices that utilize polymer-dispersed liquid crystals [32].

In the case of PIBMA it was a surprise to us that the structure observed in the nematic phase was characterized by uniform alignment of the director parallel to the axis of the cylindrical cell (see Fig. 4). This is because this polymer was shown to provide perpendicular anchoring in supramicrometer polymer-dispersed liquid-crystal droplets via optical microscopy [22], and homeotropic anchoring conditions when treated on planar glass substrates using conoscopy [33]. In the isotropic phase, it was found that the upper bound of G is very weak as a consequence of the small order parameter at the cavity wall. This suggests that the parallel alignment in the nematic phase could be a result of the weak finite anchoring energies becoming overwhelmed by elastic energies in these submicrometer channels, tilting the molecule at the surface away from their preferred perpendicular orientation to a parallel orientation. In the isotropic phase, the molecules could return to their preferred perpendicular orientation. If this is the case in our PIBMA–5CB-βd_2 system, the order parameter reported in Table I would change by a factor of 2, becoming $S_0 = 0.012$.

ACKNOWLEDGMENTS

The authors wish to acknowledge support of the National Science Foundation under Solid State Chemistry Grant No. DMR-88-17647 and ALCOM Science and Technology Grant No. DMR-89-20147. The deuterated compound 5CB-βd_2 and 10CB-d_3 was synthesized by Sandra Keast and resource facility supported under the National Center for Integrated Technology DARPA Contract No. MDA972-90-C-0037. The exchange program between Kent State University and Universität Leipzig is acknowledged. Helpful discussions with Daniele Finotello are acknowledged.

*Permanent address: Universität Leipzig, Sektion Physik, Linnestrasse 5, O-7010 Leipzig, Germany.

[1] P. G. de Gennes, Rev. Mod. Phys. **57**, 827 (1985).
[2] P. Sheng, Phys. Rev. Lett. **37**, 1059 (1976); Phys. Rev. A **26**, 1610 (1982).
[3] D. W. Allender, G. L. Henderson, and D. L. Johnson, Phys. Rev. A **24**, 1086 (1981).
[4] A. Mauger, G. Zribi, D. L. Mills, and J. Toner, Phys. Rev. Lett. **53**, 2485 (1984).
[5] A. K. Sen and D. E. Sullivan, Phys. Rev. A **35**, 1391 (1987).
[6] T. J. Sluckin and A. Pioniewierski, in *Fluids of Interfacial Phenomena,* edited by C. A. Croxton (Wiley, New York, 1986), Chap. 5, and references therein.
[7] M. M. Telo da Gamma, Mol. Phys. **52**, 585 (1984); **52**, 611 (1984); Phys. Rev. Lett. **59**, 154 (1987).
[8] K. Miyano, Phys. Rev. Lett. **43**, 51 (1979); J. Chem. Phys. **71**, 4108 (1979); J. Tarczon and K. Miyano, *ibid.* **73**, 1994 (1980).
[9] W. Chen, L. J. Martinez-Miranda, H. Hsiung, and Y. R. Shen, Phys. Rev. Lett. **62**, 1860 (1989).
[10] Y. R. Shen, Liq. Cryst. **5**, 635 (1989); P. Guyot-Sionnest, H. Hsiung, and Y. R. Shen, Phys. Rev. Lett. **57**, 2963 (1986).
[11] R. Barbero and G. Durand, Phys. Rev. A **41**, 2207 (1990).
[12] H. Yokoyama, S. Kobyashi, and H. Kamei, J. Appl. Phys. **61**, 4501 (1987).
[13] F. M. Aliev and K. S. Pozhivilko, Pis'ma Zh. Eksp. Teor. Fiz. **49**, 271 (1989) [JETP Lett. **49**, 308 (1989)].
[14] G. P. Crawford, D. K. Yang, S. Žumer, and J. W. Doane, Phys. Rev. Lett. **66**, 723 (1991).
[15] J. W. Doane, A. Golemme, J. L. West, J. B. Whitehead, Jr., and B.-G. Wu, Mol. Cryst. Liq. Cryst. **165**, 511 (1988).
[16] P. G. de Gennes, *The Physics of Liquid Crystals* (Oxford University Press, London, 1974).
[17] P. G. de Gennes, Mol. Cryst. Liq. Cryst. **12**, 193 (1971).
[18] J. W. Doane, in *Magnetic Resonance of Phase Transition,* edited by F. J. Owens, C. P. Poole, Jr., and H. A. Farach (Academic, New York, 1979), Chap. 4.
[19] M. Vilfan, V. Rutar, S. Žumer, G. Lahajnar, R. Bline, J. W. Doane, and A. Golemme, J. Chem. Phys. **89**, 579 (1988).
[20] Anotec Separations, 226 East 54th St., New York, NY 10022.
[21] J. Hoffmann, Am. Lab. **21**, 70 (1989).
[22] G. P. Crawford, D. K. Yang, and J. W. Doane (unpublished).
[23] S. Keast and M. Neubert (private communication).
[24] G. P. Crawford, M. Vilfan, I. Vilfan, and J. W. Doane, Phys. Rev. A **43**, 835 (1991).
[25] G. P. Crawford, D. W. Allender, J. W. Doane, M. Vilfan, and I. Vilfan, following paper, Phys. Rev. A **44**, 2570 (1991).
[26] J. William Doane, MRS Bull. **XVII**, 22 (1991).
[27] A. Golemme, S. Žumer, and J. W. Doane, Phys. Rev. A **37**, 559 (1988).
[28] G. Chidichimo, S. Yaniv, N. A. Vaz, and J. W. Doane, Phys. Rev. A **25**, 25 (1982).

[29] H. J. Coles, Mol. Cryst. Liq. Cryst. **49**, 67 (1978).
[30] A. Golemme, S. Zumer, D. W. Allender, and J. W. Doane, Phys. Rev. Lett. **61**, 1937 (1988).
[31] David W. Allender (private communication).
[32] J. W. Doane, in *Liquid Crystal Displays: Applications and Uses,* edited by B. Bahadur (World Scientific, Teaneck, NJ, 1990), Chap. 14.
[33] D. S. Fredley and J. L. West (private communication).

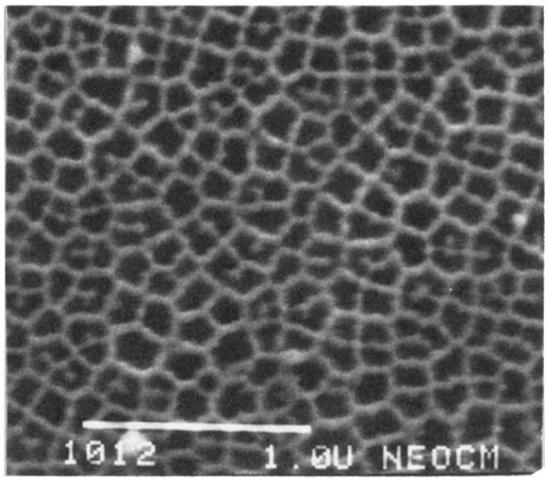

FIG. 1. Scanning-electron-microscope photograph of an Anopore inorganic membrane with pores of diameter 0.2 μm. The scale shown in the photograph represents 1 μm.